Effect of the cluster size in modeling the H_2 desorption and dissociative adsorption on Si(001)

E. Penev, P. Kratzer, and M. Scheffler
Fritz-Haber-Institut der Max-Planck-Gesellschaft, Faradayweg 4-6, 14195 Berlin-Dahlem, Germany

(Received 10 September 1998; accepted 10 November 1998)

Three different clusters, Si_9H_{12}, $Si_{15}H_{16}$, and $Si_{21}H_{20}$, are used in density-functional theory calculations in conjunction with *ab initio* pseudopotentials to study how the energetics of H_2 dissociative adsorption on and associative desorption from Si(001) depends on the cluster size. The results are compared to five-layer slab calculations using the same pseudopotentials and high quality plane-wave basis set. Several exchange-correlation functionals are employed. Our analysis suggests that the smaller clusters generally overestimate the activation barriers and reaction energy. The $Si_{21}H_{20}$ cluster, however, is found to predict reaction energetics, with $E_a^{\mathrm{des}}=56\pm3$ kcal/mol (2.4 ±0.1 eV), reasonably close (though still different) to that obtained from the slab calculations. Differences in the calculated activation energies are discussed in relation to the efficiency of clusters to describe the properties of the clean Si(001)-2×1 surface. © *1999 American Institute of Physics.* [S0021-9606(99)70307-7]

I. INTRODUCTION

Cluster models are a frequently used tool for studying different aspects of physics and chemistry of clean surfaces, adsorption, and surface chemical reactions. An example which attracted considerable experimental and theoretical interest over the last years is the H dissociative adsorption and associative desorption on the Si(001)-2×1 surface[1] which is a subject of this study. The intriguing experimental result that the H_2 desorption from Si(001) follows first-order kinetics[2–4] has triggered an intense theoretical activity in this field mainly concentrated on the mechanism(s) leading to such an unusual behavior. The available first principles calculations address the latter question on the basis of two different models: (i) the cluster approximation using either configuration-interaction (CI) methods[5–12] or density-functional theory (DFT), Refs. 8 and 13, to describe the exchange and correlation effects or (ii) extended slab models for the Si(001)-2×1 surface using DFT.[14–16]

The DFT slab calculations all agree in their conclusions supporting the *prepairing* mechanism[3] according to which two hydrogens are prepaired on the same Si surface dimer and associatively desorb through an asymmetric transition state (TS). The cluster calculations, however, have led to different conclusions. All these calculations find a rather high barrier for desorption of two hydrogens from a single Si dimer, e.g., $E_a^{\mathrm{des}}=$ 74–75 kcal/mol (3.2 eV),[8] 85–86 kcal/mol (3.7 eV),[10] 82–85 kcal/mol (3.6–3.7 eV).[12] Comparing to the experimental activation energy of desorption of ~58 kcal/mol (2.5 eV),[3,4,17,18] these findings were interpreted as being compelling evidence against the prepairing mechanism. In an attempt to reconcile the experimentally observed energetics and kinetics of desorption from the monohydride phase, various defect-mediated mechanisms[6–8,12] were suggested including formation of metastable dihydride species as an intermediate step. All the above studies have in common that their argumentation rests on computational schemes based on CI and the small and simple Si_9H_{12} cluster to model the Si(001)-2×1 surface except the work by Nachtigall *et al.*,[8] where DFT has been employed. In some studies larger clusters, like $Si_{16}H_x$ (Ref. 8) or $Si_{21}H_x$,[19] have been used. Nevertheless, the effect of cluster size on the energetics of H_2 adsorption/desorption on Si(001) has not been analyzed in detail in the literature.

The only cluster-based support to direct desorption via the prepairing mechanism comes from the DFT calculations by Pai and Doren.[13] Using the nonlocal Becke-Lee-Yang-Parr (BLYP) functional,[20,21] they find $E_a^{\mathrm{des}}=64.9$ kcal/mol (2.8 eV) including a zero-point energy (ZPE) correction. Given the uncertainties originating both from the use of different functionals and from inherent limitations of the cluster approximation, they considered their result to be compatible with the experimental desorption energy. The first possible source of error, the reliability of the functional, was addressed by Nachtigall *et al.*,[11] who systematically compared various density functionals to the results of the state-of-the-art computational tool in quantum chemistry, an extrapolated quadratic CI method. For the sake of computational feasibility, they concentrated on a few simple test cases, four reactions involving silanes, and a Si_2H_6 cluster with a geometry chosen to mimic H_2 desorption from Si(001). While the extrapolated quadratic CI method gives a reference value of 90.4 kcal/mol (3.92 eV) for E_a^{des}, the Perdew-Wang (PW91) functional[22] underestimates E_a^{des} by 9.5 kcal/mol (0.41 eV) compared to this reference. The Becke-Perdew (BP) functional[20,23] gives an even lower barrier, $E_a^{\mathrm{des}}=79.4$ kcal/mol (3.44 eV). Generally, Nachtigall *et al.* find the B3LYP functional[24] to give closest agreement with their CI calculations, while the BLYP functional is performing second best. A similar trend concerning the performance of different functionals was also observed in the case of H diffusion on the Si(001)-2×1 surface.[25] However, we find it not to be *a priori* clear whether their conclusions could be ap-

 © 1999 American Institute of Physics

plied to better cluster approximations to the Si(001) surface, because the electronic wave functions at a surface are generally more extended than in a cluster and this may naturally affect the electron-electron correlations. It is one of the aims of the present paper to study the performance of different functionals with the size of the clusters.

A second issue which hampers a clear-cut comparison of different approaches lies in the geometric structure of the clean Si(001) surface. While the DFT calculations give the correct description of the geometry of the clean surface, normally a $p(2\times2)$ or $c(4\times2)$ reconstruction with buckled Si dimers,[26,27] CI calculations predict a symmetric ground state of the clusters. This could imply substantial differences between the two approaches in the surface relaxation during the adsorption/desorption process as well as in the surface electronic structure. Since H_2 dissociation on Si(001) is known to couple to the surface motion,[28,15,16] one could expect these differences in the description of the clean Si(001) surface also to influence the reaction energetics predicted by different calculational approaches.

In the light of the above we find of particular interest to bridge the DFT slab and cluster calculations by studying the convergence of the H_2 adsorption/desorption energetics with cluster size. Since the results of the DFT calculations agree about a direct desorption process and the very recent experiment by Flowers *et al.*[29] also supports this mechanism, we shall perform our analysis adopting the prepairing scenario for the Si(001) surface. A description of the computational method used in the present work is given in the next section. In Sec. III particular attention is paid to the structure of the clean Si(001) surface. Clusters with one, two and three surface dimers are used in Sec. IV to study the energetics of the adsorption/desorption process. A summary of the results and discussion is presented in the last section.

II. CALCULATIONS

A. The systems used for modeling H_2/Si(001)

Generally, cluster models for surface chemical processes are treated in conjunction with a basis set for the electronic states consisting of localized orbitals. However, special care is required in choosing a basis set which meets the desired level of accuracy. In order to isolate the different approximations inherent in the choice of the cluster and the basis set size, we decide to perform total energy calculations within the DFT scheme as implemented in the FHIMD package,[30] employing a plane waves basis set with well-controlled convergence properties. We report results for the three different clusters shown in Fig. 1(a), Si_9H_{12}, $Si_{15}H_{16}$ and $Si_{21}H_{20}$. Each of them represents the topmost four layers of the reconstructed surface. They differ by the number of Si-Si surface dimers they contain. The larger $Si_{15}H_{16}$ and $Si_{21}H_{20}$ clusters are derived from Si_9H_{12} by adding one and two dimers, respectively, in the $[1\bar{1}0]$ direction along with their full coordination of second layer Si atoms, one third and one fourth layer Si atom. All dangling bonds of the silicons in the subsurface layers are saturated with hydrogen atoms. By increasing the cluster size in this way we aim at reaching three ascendingly improved approximations to the clean Si(001)

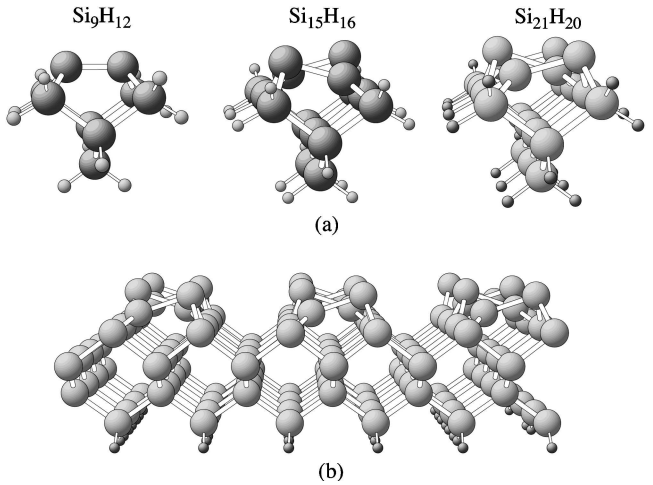

FIG. 1. BP optimized geometries of (a) the clusters used to model the Si(001)-2×1 surface and (b) the five-layer $p(2\times2)$ slab used as a reference system.

surface: Si_9H_{12} is the minimal one to represent the symmetric 2×1 reconstruction; $Si_{15}H_{16}$ is the smallest cluster that enables to model the $p(2\times2)$ surface reconstruction. Finally, $Si_{21}H_{20}$ contains one surface dimer surrounded by two others, thus having the same local environment as on the surface. In the context of H_2 desorption from the monohydride phase, the larger clusters also allow us to study the interaction between adjacent occupied dimers.

Since the super cell approach implemented in FHIMD implies periodic boundary conditions for the wave functions, the clusters are placed in a sufficiently large orthorhombic unit cell, where they are separated by ≈7 Å to avoid unwanted interactions. Since the electronic states of the cluster Hamiltonian have no dispersion, it is sufficient to calculate them at a single point in the Brillouin zone (BZ), $\mathbf{k}_\Gamma = (0,0,0)$.

To link the current discussion with the available slab calculations, we perform as a final step a set of calculations employing a $p(2\times2)$ slab with five Si layers, Fig. 1(b), similar to Ref. 15. The *k*-space integration is performed using 16 $\mathbf{k}_\parallel$ points in the whole surface Brillouin zone of the 2×2 unit cell.

Both cluster and slab calculations are carried out using the local-density approximation (LDA) to the exchange-correlation functional, as obtained form the Monte Carlo results by Ceperley and Alder[31] in the parameterization of Perdew and Zunger.[32] For comparison all calculations are repeated with gradient corrections as described by the BP, PW91 and BLYP functionals. Our choice to include these functionals in the test is partially motivated by the good agreement between previous slab calculations and the experiment, but on the other hand by the shortcomings of the BP and PW91 functionals, cf. Ref. 11, found in the case of small systems. DFT *plane-wave* calculations employing either slabs or Si_9 or larger clusters and the BLYP functional have not yet been reported for the H_2/Si(001) reaction energetics.

We employ norm-conserving *sp*-nonlocal pseudopotentials for Si atoms, generated from a separate all-electron calculation of the Si atom for each exchange-correlation

functional[33] according to Hamann's scheme.[34] For gradient-corrected DFT calculations, the use of these consistently constructed pseudopotentials ensures the proper description of core-valence exchange within each of the gradient-corrected functionals used.[35] For the hydrogens passivating Si dangling bonds, an *s*-nonlocal pseudopotential is generated following the Troullier and Martins prescription.[36] However, for the hydrogen atoms taking part in the reaction, we employ the full $1/r$ potential. For all energies quoted in the paper, plane waves with a kinetic energy up to $E_{\mathrm{cut}}=30$ Ry (408 eV) were included in the basis set. While geometries and relative energies for systems consisting entirely of Si atoms are well converged already at 18 Ry (245 eV), the high quality basis set is required for a correct description of the hydrogen wave functions close to the core.

B. Structure optimization

We perform separate structure optimizations for each cluster size and for the LDA, BP, PW91 and BLYP functionals. The first step in all structure relaxation runs was to optimize the positions of the terminating hydrogens, with the subsurface silicon coordinates kept fixed at their bulk values, and the symmetric dimer bond length set to $d=2.28$ Å as found in Ref. 16.

One of our present goals is to investigate to what extent clusters are appropriate for a description of the Si(001) surface. One important feature of the clean surface is the buckling of the Si surface dimers (see the next section). It is therefore interesting to test if the buckling can be modeled by clusters of appropriate size. The failure of small clusters to reproduce the buckled surface structure is sometimes attributed to the neglect or underestimate of elastic interactions between Si dimers in this approach. However, the importance of elastic interactions is established only for the alternation of buckling angle (''antiferromagnetic ordering'') in the $p(2\times2)$ or $c(4\times2)$ reconstruction.[37] To distinguish elastic from electronic effects, we employ a two-step procedure to determine the equilibrium structures of the bare clusters. First we sample the total energy as a function of the dimer buckling angle α, as done, for example, in Refs. 16,26, but without relaxation of any of the deeper layers. Thus any elastic interactions between Si dimers are avoided. Neighboring dimers (if there are any) are buckled in opposite directions, with buckling angles α and $-\alpha$, to mimic the $p(2\times2)$ surface reconstruction.

The structure of the bare clusters is finally determined by unconstrained relaxation of the topmost two Si layers. Here we use the energy minimum as a function of α determined in the previous calculations as input for the starting geometry. The two pairs of hydrogens saturating the second layer Si bonds in the $[1\bar{1}0]$ direction, which would correspond to adjacent Si dimers on the Si(001) surface, are also allowed to relax. We have also tested full relaxation of all layers in the case of the Si_9H_{12} and $Si_{15}H_{16}$ clusters within LDA. The lack of any geometric constraints, however, tends to overestimate the surface relaxation and introduces unrealistic atomic displacements. Full relaxation would only be appropriate for clusters studied as objects in their own interest, rather than as an approximation to the Si(001) surface.

The structure of the monohydride phase is determined by relaxing the adsorbate and the two Si layers beneath it. In the case of the Si_{21} cluster the H_2 molecule is adsorbed on the middle dimer. The geometries of transition states (TS) are determined by a search algorithm using the ridge method proposed by Ionova and Carter.[38] Since geometries are less sensitive to the quality of the basis set than the total energies, we have found it sufficient to perform geometry optimizations at a plane-wave cut-off of $E_{\mathrm{cut}}=18$ Ry. The structures are considered converged when all forces are smaller than 0.05 eV/Å .

III. THE CLEAN Si(001)-2×1 SURFACE

On the Si(001) surface, the surface Si atoms form dimers, leading to the (symmetric) 2×1 reconstruction. The surface can reduce its symmetry if the Si surface atoms relax to different heights, i.e., the dimers are buckled. This leads to the formation of lower symmetry patterns, the asymmetric $p(2\times1)$, $p(2\times2)$, $c(4\times2)$. These reconstructions are characterized by the dimer buckling angle α, the dimer bond length d, and the energy favor per dimer ΔE with respect to the symmetric 2×1 reconstruction.

The calculations for H_2 desorption from Si(001) using slabs together with DFT and those based on many-body wave functions (like CI) already differ in their description of the clean surface geometry. In the latter calculations, mostly the Si_9H_{12} cluster with one symmetric Si dimer was used as reference state for the clean Si(001) surface. Radeke and Carter verified that the symmetric cluster is the geometric ground state at the level of theory used in their work.[12] Recent theoretical studies[39–41] on Si clusters come to conflicting conclusions and thus leave the discussion about the ground state symmetry of Si clusters still open.

On the other hand, the DFT slab calculations[15,16,26,42,43] are consistent in their predictions and show good agreement with recent experiments. Direct evidence for the buckling comes from low-temperature STM images[27] and structure determinations by LEED.[44] Furthermore, observed core-level shifts[45] are inconsistent with symmetric surface dimers, but can be explained by buckled dimers.[46] The buckled surface reconstruction has gained further support by the good agreement between the measured dispersion of surface band states[47] with calculations using the GW approximation.[48]

The different symmetries of reconstruction correspond to different electronic structures at the surface. Previous theoretical work[15,43,49] has established the following picture: After dimerization of the surface Si atoms, they would both remain to have dangling bonds occupied by one electron, i.e., a degenerate electronic ground state. There are two principal possibilities for a lowering of the electronic energy. First, a bonding and antibonding linear combination of orbitals could be formed (similar to a π-bond in a free dimer), only one of which is occupied. In this case the Si surface dimer would remain symmetric. The second possibility is a Jahn-Teller-type splitting of the degeneracy. By buckling the Si dimer, the lower Si atom comes to an almost planar bonding configuration with its three neighbors, while the upper Si atom

reaches a pyramidal configuration. A rehybridization of the orbitals at each of the Si atoms results in a lowering of the dangling orbital at the upper Si atom, and in an up-shift of the orbital at the lower Si atom, which is accompanied by a transfer of electron density from the lower to the upper atom. The preferred way of stabilization depends on several factors: the possible strength of the π-bond, the possible energy gain due to rehybridization, the ability of the system to screen the increased Coulomb repulsion in the dangling bond of the upper Si atom, and the energetic cost of elastic deformation in the deeper layers induced by the buckling. The ground state geometry is thus determined by an interplay of both elastic and electronic effects and could be quite sensitive to different surface reconstructions and computational methods.

Before we describe our own results for the ground state of clusters, we briefly discuss the recent literature. Yang *et al.*[40] do not find buckling for the Si_9H_{12} cluster, either within Hartree-Fock or in a DFT calculation employing the B3LYP functional. Increasing the cluster size to $Si_{15}H_{16}$, however, unambiguously shows an energy favor for the buckled $p(2\times2)$ reconstruction, ~3–5 kcal/mol (0.15–0.23 eV) per dimer depending on the basis set used. Konečný and Doren[39] have used the same cluster and the BLYP functional to study H_2O adsorption on Si(001)-2×1 and found a buckled dimer structure for Si_9H_{12} with $\alpha=9.6°$, $\Delta E=0.05$ kcal/mol (0.002 eV) and $d=2.27$ Å while for the two-dimer cluster $Si_{15}H_{16}$ they obtained $\alpha=15°$, $\Delta E=1.5$ kcal/mol (0.07 eV) per dimer and $d=2.33$ Å . The two research groups use different relaxation constraints and basis sets. This could explain the differences, given that a delicate balance of several effects is responsible for the ground state configuration of the Si_9H_{12} cluster.

In the present study, the ground state of the clusters is determined in a two-step procedure. In the first step, the Si dimers are tilted as a whole, while keeping the other cluster atoms fixed and preserving the length of the dimer backbonds. We sample the total energy as a function of the dimer buckling angle α. The results for LDA and the PW91 functional are shown in Fig. 2. They are summarized in the ''prerelaxation'' column of Table I for all functionals used in the calculations.

The ΔE vs α curves are mainly affected by the cluster size, rather than by the approximation used for exchange and correlation. Upon increasing the cluster size, the minima become well pronounced and are shifted to larger α values, the upper bound being set by $\alpha^{(\mathrm{LDA})}$. In the case of Si_9H_{12}, $\alpha=0$ is the only minimum when using the BP and BLYP functionals. The values obtained within LDA and PW91 for this cluster are small. Thus the Si_9H_{12} cluster gives no conclusive answer to the question whether the Si surface dimers are buckled or not. The larger clusters, however, clearly show a preference for buckling. Since we have frozen the elastic degrees of freedom, the only driving force that can lead to dimer buckling is rehybridization and charge transfer. The prerelaxation study supports the view that surface dimer buckling is mainly driven by electronic effects, while elastic effects are responsible for the alternation of the buckling angle.

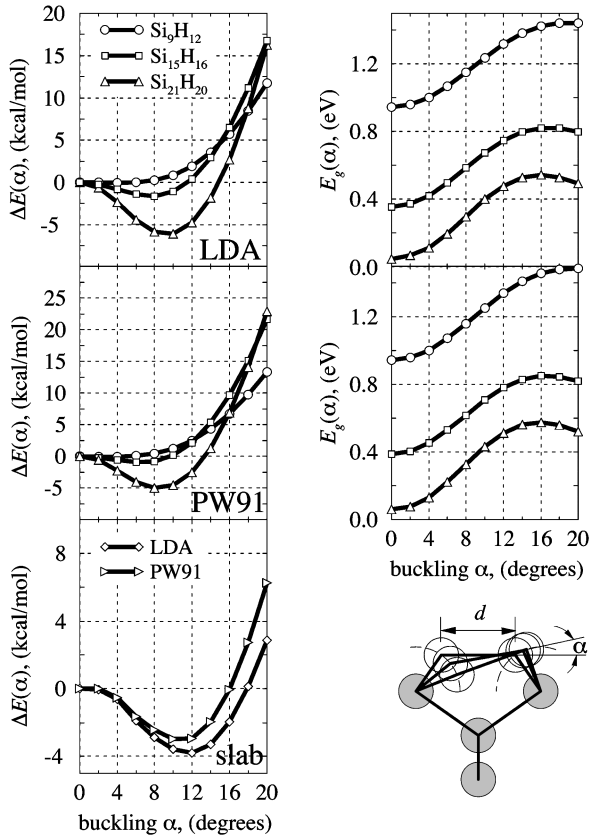

FIG. 2. Total energy preference $\Delta E=E(\alpha)-E_0$ (left column) and the gap $E_g(\alpha)$ between HOMO and LUMO (right column) for the clusters as a function of dimer buckling angle α. The bottom left panel shows $\Delta E(\alpha)$ for the five-layer $p(2\times2)$ slab. E_0 is taken to be the energy of the corresponding unrelaxed symmetric ($\alpha=0$) cluster/slab for a given exchange-correlation functional. Buckling is achieved by gliding the two dimer Si atoms along arcs (dashed lines) as shown in the inset (bottom-right panel) and keeping all other atoms fixed (shaded circles).

The electronic structure of the cluster is influenced substantially by the dimer buckling. As a measure of the differences, we report the splitting between the highest occupied and lowest unoccupied molecular orbitals (HOMO and LUMO) of the cluster, E_g, in the right column in Fig. 2. For Si_9H_{12} E_g is a monotonically increasing function of α. It reaches its maximum for the largest used value of $\alpha=20°$, where the two dimer silicons and the two second layer neighbors of the buckled-down Si atom are almost coplanar. We attribute the opening of the HOMO-LUMO gap to changes in the symmetry character of the orbitals. While at $\alpha=0$ the HOMO and LUMO orbital correspond to the π and π^* orbital of the Si dimer, they gradually develop into orbitals localized at one side of the Si dimer for increasing α. The orbital at the lower Si atom acquires more p-character and is lifted in energy, while the orbital at the higher Si atom gets more s-character and is energetically lowered.[49] With increasing cluster size E_g is strongly reduced, while the dependence on α is almost unchanged. For the larger clusters we observe that the HOMO (LUMO) wave functions are no longer localized at a single Si atom, but are linear combinations of the dangling orbitals of all the buckled-up (buckled-down) Si atoms of the cluster. In the $Si_{21}H_{20}$ cluster, this leads to a splitting of the HOMO and LUMO levels into

TABLE I. Parameters of the clusters and the slab for different exchange-correlation functionals; the energy favor for buckling ΔE is given in kcal/mol per dimer and the gap E_g between HOMO and LUMO in eV. d refers to the Si-Si dimer bond length in Å and α to its buckling angle in degrees.

	Prerelaxation			Two layers relaxed[a]			
	α	$\lvert\Delta E\rvert$	E_g	α	$\lvert\Delta E\rvert$	E_g	d
LDA							
Si_9	4	0.1	1.00	6.9	0.1	1.18	2.21
Si_{15}	8	0.8	0.59	15.7	2.7	0.86	2.28
Si_{21}	10	2.0	0.40	18.6	4.0	0.70	2.35
slab	12	1.9		18.9	4.5		2.36
BP							
Si_9	0	—	0.99	0	—	0.96	2.27
Si_{15}	6	0.4	0.54	15.3	2.6	0.86	2.37
Si_{21}	8	1.4	0.33	18.1	4.4	0.78	2.47
slab	10	1.3		18.6	5.1		2.46
PW91							
Si_9	2	0.0	0.96	4.9	0.1	1.10	2.24
Si_{15}	6	0.5	0.43	15.7	3.1	0.88	2.32
Si_{21}	8	1.7	0.33	18.0	4.6	0.74	2.40
slab	10	1.5		18.3	5.1		2.40
BLYP							
Si_9	0	—	1.02	0	—	0.99	2.27
Si_{15}	4	0.1	0.51	12.2	1.6	0.72	2.33
Si_{21}	6	0.8	0.27	16.6	3.5	0.72	2.44
slab	10	0.8		16.6	4.7		2.43

[a]α and d for the $Si_{21}H_{20}$ cluster correspond, respectively, to the buckling angle and bond length of the middle dimer.

symmetric and antisymmetric states with respect to the mirror plane in the cluster, Fig. 3. Thus this cluster reflects already to some extent the dispersion of surface bands observed in the slab. We expect that these changes in the electronic structure will also be reflected in the chemical reactivity, i.e., in the adsorption barrier E_a^{ads} for H_2 molecules. It appears that a representation of the surface band structure on the cluster level is required for a correct description of the reaction energetics.

Relaxing the first and second silicon layers does not qualitatively change the results from the prerelaxation study. However, the ground state energy and geometry differ substantially. The buckled dimer configurations of the $Si_{15}H_{16}$ and the $Si_{21}H_{20}$ clusters are now more stable by 1.5–3 kcal/mol (0.07–0.13 eV) and 3.5–4.5 kcal/mol (0.15–0.20 eV) per dimer, respectively. The HOMO-LUMO gap is found to decrease with increasing cluster size. The reduction can be partly attributed to a splitting of both the HOMO and LUMO state due to linear combinations of dangling bonds at neighboring Si dimers in the larger clusters (see Fig. 3). However, a decrease is also observed, in particular at $\alpha=0$, for a suitably averaged gap $\langle E_g\rangle$, defined as

$$\langle E_g(\alpha)\rangle_N=\frac{1}{N}\sum_{j=0}^{N-1}\left[E_{\mathrm{LUMO}+j}(\alpha)-E_{\mathrm{HOMO}-j}(\alpha)\right],$$

where N is the number of dimers in the cluster. The reduction of the gap must be attributed to a weakening of the π-bonding with increasing cluster size. As could be anticipated, $Si_{21}H_{20}$ gives closest agreement with the five-layer $p(2\times2)$ slab. The Si_9H_{12} cluster, on the contrary, is not large enough to model the properties of the clean Si(001)-2×1 surface. Buckling in this case is strongly influenced by relaxation constraints and the approximation to exchange and correlation. While for the two larger clusters all functionals used here give similar results, their predictions for the Si_9H_{12} ground state symmetry are qualitatively different. Though LDA and PW91 favor buckling with $\alpha\approx7°$ and 5°, respectively, $\lvert\Delta E\rvert$ is too small ($\sim$0.1 kcal/mol) to allow us to conclude unequivocally about the Si_9H_{12} cluster symmetry.

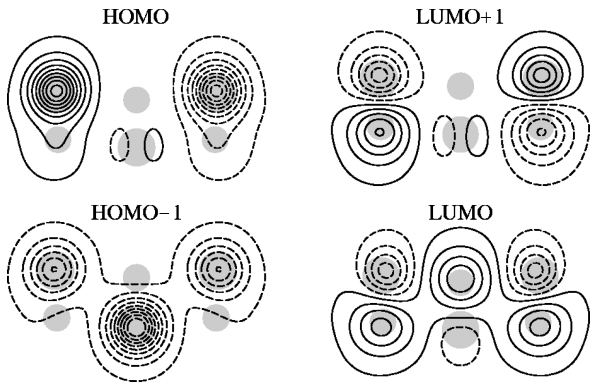

FIG. 3. Top view of the $Si_{21}H_{20}$ cluster frontier orbitals. The contour plots are taken in the (001) plane 0.9 Å above the buckled-up Si atom of the middle dimer (dimers are denoted by shaded circles). The wave functions are real-valued. Full (dashed) contour lines indicate positive (negative) sign.

For the two-dimer $Si_{15}H_{16}$ cluster using the BLYP functional we get d and ΔE values identical to those of Konečný and Doren, but their predicted Si_9H_{12} geometry is at variance with ours. Possibly the overestimation of the surface relaxation due to the absence of any geometric constraints in Ref. 39 is more crucial for the Si_9H_{12} cluster than for the larger ones.

At our imposed relaxation constraints the BP and BLYP functionals are found to give results for Si_9H_{12} in agreement with the CI methods.[12,41] For the $Si_{15}H_{16}$ cluster, however, buckling is always energetically favorable within DFT, whereas recent multireference CI calculations[41] find the symmetric cluster to be lowest in energy. At present it is not clear if this is due to a lack of the CI calculations to recover the full correlation energy, or due to an inadequacy of the exchange-correlation functionals we are using. For the largest $Si_{21}H_{20}$ cluster, we are not aware of CI calculations addressing the dimer buckling.

IV. REACTION ENERGETICS

The energetics of dissociative adsorption and associative desorption of H_2 is characterized by three points along the reaction pathway, the energies of the structures corresponding to the monohydride phase E_{11}, the transition state energy E_{TS} and the sum of bare cluster energy E_{00} and that of the free H_2 molecule. Hence, the quantities of interest are defined by the differences

$$E_a^{\mathrm{ads}}=E_{\mathrm{TS}}-(E_{00}+E(\mathrm{H_2})),$$

$$E_a^{\mathrm{des}}=E_{\mathrm{TS}}-E_{11},$$

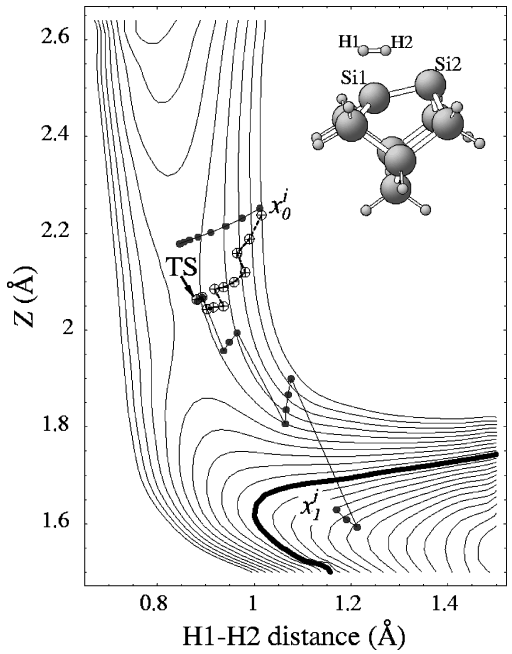

FIG. 4. Sketch of the ridge method search for TS and the adiabatic PES for the Si_9 cluster within LDA. Crossed circles ($\oplus$) denote the successive approximations to the TS. The contour spacing is 0.05 eV and the energy is measured with respect to $E_{00}+E(H_2)$ (solid contour line). The transition state geometry is shown in the inset. The PES is plotted for H_2 molecule impinging perpendicularly to the surface with its center of mass right above the Si1 site, Z being the distance between them.

$$E_{\mathrm{rxn}}=E_{00}+E(H_2)-E_{11}.$$

The monohydride geometry of each cluster is obtained by saturating the dangling bonds of one Si dimer with H atoms. The equilibrium Si-H bond is 1.52 Å within LDA, PW91 and BLYP. When using the BP functional a bond length larger by 0.03 Å is obtained. The changes in d of the hydrogenated dimer are mainly governed by the approximation to the exchange and correlation, while the cluster size accounts only for differences of ~0.01 Å for a given functional. We note that our TS and monohydride structures imply reaction of a single H_2 molecule with the Si(001) surface. For comparison to experimental data taken at finite hydrogen coverage, information about the coverage dependence of the energetics is also required. A single H_2 molecule per $p(2\times2)$ unit cell in the extended slab case corresponds to a coverage of $\Theta=0.5$ monolayers (ML). To assess the coverage dependence of the reaction energy E_{rxn}, test calculations were carried out for a completely covered slab, $\Theta=1$ ML. To obtain a better understanding of the role of buckling for the reaction energetics, we also performed test calculations for the symmetric $p(2\times1)$ reconstructed Si(001) surface as possible reference of the clean surface. We note that the occupation of adjacent Si dimers by hydrogens could have a (probably small) influence on the transition state geometries and energies via interaction with the neighboring monohydride. This effect can be studied to some extent with the help of the two- and three-dimer clusters, which allow for adjacent doubly occupied Si dimers. To get some insight into the influence of neighboring monohydrides on the asymmetric TS, we have performed calculations with $Si_{15}H_{16+x}$ and $Si_{21}H_{20+x}$ clusters with $x=4$ and 6, respectively.

In this study, we concentrate on the prepairing scenario for the H_2 reaction with the Si(001) surface. Consequently, we locate the asymmetric TS of H_2 desorption from a single Si dimer for all clusters and functionals used in this study. In principle this can be achieved by mapping out the related potential-energy surface (PES), like e.g., in Ref. 15. As an example, the potential energy as a function of the distance between the two H atoms and the H_2-cluster distance Z is shown in Fig. 4. For each configuration of the two H atoms, the Si atoms in the two topmost layers have been relaxed. They follow ''adiabatically'' the motion of the H atoms. Thus we make sure that the lowest possible TS in the multidimensional space of all mobile atomic coordinates is found. An alternative and generally faster approach uses a search algorithm, thus avoiding the need to map out all the points in the PES. All degrees of freedom of the H_2 molecule and the topmost two cluster/slab Si layers are included in the search. The ridge method[38] implemented here starts from a pair of coordinates x_0 and x_1 in the multidimensional configuration space of the system, which denote the reactants (H_2 above the bare surface) and the products (the monohydride), respectively. An iterative search is then performed by halving the interval $[x_0,x_1]$ in some steps. To reduce the number of required steps, we have shifted the input coordinates towards some initial guess (x_0^i,x_1^i) closer to the TS. A projection of the search path onto a two-dimensional slice of the coordinate space is shown in Fig. 4 for the Si_9H_{12+2} cluster within LDA. As seen, there is excellent agreement between the two schemes.

The geometries of the calculated TS are collected in Table II. As expected, the H-H bond is stretched in the asymmetric TS configuration of all Si_xH_{y+2} clusters, with $R_{\mathrm{H1\text{-}H2}}$ being largest for dissociation on the Si_{21} cluster. As a consequence, the atom H2 at the transition state is by 0.2–0.3 Å closer to the buckled-up Si2 atom as compared with the Si_9 cluster. The presence of two H atoms over the Si1 site partially blocks the mechanism that leads to anticorrelated dimer buckling and therefore $\alpha_{\mathrm{TS}}<\alpha$. For the Si_{21} cluster the unoccupied dimers are somewhat affected by the adsorption event, but their buckling angle α' is only a few degrees smaller than that of the clean surface. This small change is due to the dimer row termination by hydrogens in the clusters, and is absent in the slab geometries, where $\alpha'\approx\alpha$.

Most noticeable in the results shown in Fig. 5 (numerical values are compiled in Table III) is a clear dependence of E_a^{ads}, E_a^{des} and E_{rxn} on cluster size. The common trend for all functionals is an effective flattening of the PES along the reaction path with increasing cluster size. Both the reaction energy and the adsorption barrier are reduced. In general, for all clusters considered here, LDA gives a lower bound for the activation barriers and an upper one for E_{rxn}. For a given size of the cluster, we can compare the effect of the exchange-correlation functional employed in the calculation. As far as E_{rxn} is concerned, all gradient-corrected functionals behave in a very similar way (see bottom panel of Fig. 5). This gives credibility to the statement that gradient-corrected

TABLE II. Transition state geometry parameters in Å (see the inset in Fig. 4). α' denotes the buckling angle in degrees of the unoccupied dimer(s) in the case of slab and Si_{15}, Si_{21} clusters.

	$R_{H1\text{-}H2}$	$R_{Si1\text{-}H1}$	$R_{Si1\text{-}H2}$	$R_{Si2\text{-}H2}$	d	α_{TS}	α'
LDA							
Si_9	0.88	2.12	2.10	2.38	2.30	13.7	—
Si_{15}	0.97	1.93	1.98	2.24	2.38	12.1	15.6
Si_{21}	1.06	1.95	2.14	2.09	2.38	13.0	15.5
slab	0.93	2.00	2.11	2.24	2.39	13.5	19.0
BP							
Si_9	0.94	1.96	1.95	2.34	2.42	12.2	—
Si_{15}	1.02	1.84	1.95	2.19	2.46	11.5	15.5
Si_{21}	1.02	1.82	2.01	2.12	2.47	11.6	14.8
slab	1.03	1.80	1.94	2.11	2.50	13.1	18.7
PW91							
Si_9	0.89	1.98	1.96	2.32	2.37	12.2	—
Si_{15}	0.99	1.84	1.94	2.19	2.40	10.7	14.6
Si_{21}	1.08	1.89	2.11	2.04	2.41	13.6	14.9
slab	0.99	1.83	1.99	2.12	2.43	12.7	18.4
BLYP							
Si_9	0.91	1.93	1.95	2.31	2.40	11.9	—
Si_{15}	0.96	1.86	1.98	2.23	2.44	10.2	12.6
Si_{21}	0.96	1.83	2.02	2.11	2.48	12.1	13.8
slab	1.02	1.74	1.89	2.12	2.48	11.1	18.4

DFT yields an accurate description of reaction energies. The quantities E_a^{ads}, E_a^{des}, involving transition state energies, show a stronger variation. The differences between BP and PW91 are only ~2 kcal/mol, with the sign depending on the size of the system. The BLYP functional gives the highest value for $E_a^{ads,\,des}$ of all tested functionals. Since similar performance has been already established for small systems[11] and the Si_9 cluster,[13] our calculations confirm these results for extended clusters and slabs.

The Si_{21} cluster displays both the lowest adsorption and desorption barriers. Comparison between this cluster and the slab shows that their predictions agree to within ~3 kcal/mol for all quantities. We conclude that the Si_{21} cluster gives a fair description of the Si(001) surface, while the others are inadequate approximations for the surface. While the desorption barriers derived from the Si_{21} cluster are in the range of 56 ± 3 kcal/mol for all functionals, E_a^{ads} is more sensitive to the functional used, with values covering a range of 11 kcal/mol. The adsorption barriers derived from the gradient-corrected functionals using this cluster are 7–11 kcal/mol higher than the LDA barrier. This is in accord with the established picture that LDA tends to underestimate adsorption barriers at surfaces.[50] We note that the Si_{21} cluster yields higher barriers for the PW91 functional than for BP, while the slab calculations give the opposite result.

It is instructive to analyze why the smaller Si_9 and Si_{15} clusters give a poor description of the physics at the Si(001) surface, despite the fact that the Si–H bond is localized and should therefore be well represented already in the smallest cluster used. For E_{rxn}, the variation with cluster size is mainly due to differences in the bare clusters which are used as reference states. The buckling of the Si dimers characteristic for the Si(001) surface only fully develops in the largest

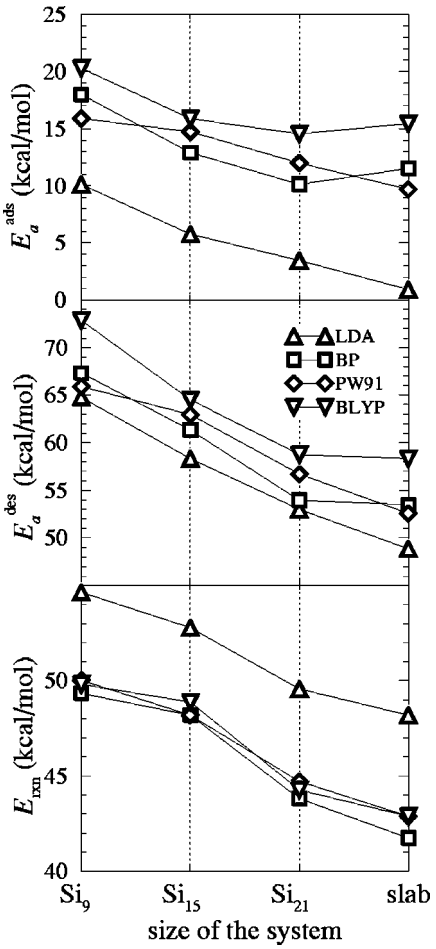

FIG. 5. H_2/Si(001) reaction energetics as a function of the size of the system used to model the Si(001)-2×1 surface (see also Table III).

clusters, because it requires a correct description of the electronic surface states. Thus nonlocal electronic effects enter the calculation of the reaction energy. They give rise to a reduction of E_{rxn} by about 5 kcal/mol compared to the value obtained with the Si_9 cluster. For E_a^{ads}, the differences between small clusters and the slab calculation are even larger. This is due to the fact that the dangling bonds of the Si dimer act as frontier orbitals in the reaction with H_2. The importance of the change in the HOMO and LUMO position that accompany dimer buckling has also been emphasized in recent first principles studies of H_2O,[39] C_2H_2,[49] BH_3,[51] and 1,3-cyclohexadien[52] reactions with the Si(001) surface. As our calculations show, the HOMO-LUMO gap E_g is substantially reduced when going from the (mainly π-bonded) Si dimer in Si_9 to the surface band states in the slab. At the transition state for adsorption, the H_2 molecular orbitals, in particular the antibonding $^3\Sigma_u$ orbital, mix with both the HOMO and LUMO orbital, which is facilitated by a small E_g. At the TS of the Si_9 cluster, the H_2 mainly interacts with one dangling bond of the lower Si atom (see Fig. 6). In the more extended systems with smaller E_g, there is also a direct interaction between the H_2 molecule and the upper Si atom. This shows up in the more localized induced charge distribution between H2 and Si2 (right panel of Fig. 6), and in the different geometrical structure of the transition state.

TABLE III. Activation and reaction energies in kcal/mol (eV) per molecule for H_2 adsorption/desorption on the Si(001)-2×1 surface via the prepairing mechanism (ZPE not included).

	E_a^{ads}	E_a^{des}	E_{rxn}
LDA			
Si_9	10.2 (0.44)	64.9 (2.81)	54.7 (2.37)
Si_{15}	5.7 (0.25)	58.4 (2.53)	52.7 (2.29)
Si_{21}	3.5 (0.15)	53.1 (2.30)	49.6 (2.15)
slab	0.9 (0.04)	49.0 (2.12)	48.1 (2.09)
BP			
Si_9	18.1 (0.78)	67.3 (2.92)	49.3 (2.14)
Si_{15}	13.3 (0.56)	61.4 (2.66)	48.1 (2.09)
Si_{21}	10.2 (0.44)	53.9 (2.34)	43.8 (1.90)
slab	11.6 (0.50)	53.4 (2.32)	41.8 (1.81)
PW91			
Si_9	15.9 (0.69)	66.0 (2.86)	50.1 (2.17)
Si_{15}	14.8 (0.64)	63.0 (2.73)	48.2 (2.09)
Si_{21}	12.0 (0.52)	56.7 (2.46)	44.7 (1.94)
slab	9.6 (0.42)	52.5 (2.28)	42.9 (1.86)
BLYP			
Si_9	20.2 (0.88)	72.8 (3.16)	49.7 (2.16)
Si_{15}	15.8 (0.69)	64.6 (2.80)	48.8 (2.12)
Si_{21}	14.5 (0.63)	58.8 (2.55)	44.3 (1.92)
slab	15.5 (0.67)	58.4 (2.53)	42.9 (1.86)

The trends in the reaction energetics outlined above do not change substantially if TS and monohydride configurations of the Si_{15}, Si_{21} clusters with more than one monohydride are employed. Test calculations using $Si_{15}H_{16+4}$ and $Si_{21}H_{20+6}$ clusters show that finite coverage effects at the TS introduce a variation of less than 3 kcal/mol in the calculated barriers. The coverage dependence of E_{rxn} was studied for the slab[53] with initial coverage $\Theta=1$ ML, Table IV. It is energetically more expensive to desorb a H_2 from one of the dimers if the other stays monohydride. Thus, $E_{rxn}(1 \rightarrow 0.5\text{ML})$ is about 3–4 kcal/mol larger than E_{rxn} calculated for initial coverage $\Theta=0.5$ ML. The reaction endothermicity for the removal of a whole monolayer comes out as the average of the endothermicities associated with the removal of each of the two monohydrides in the unit cell. It is interesting to note that E_{rxn} for the Si_{21} cluster with one monohydride (see Table III) coincides with $E_{rxn}(1\text{ML})$, rather than with the low-coverage limit of the slab, $E_{rxn}(0.5\,\text{ML})$. The coverage dependence calculated for the slab shows the same trend as the experimental data by Flowers *et al.*,[29] where a slight increase of the desorption energy with coverage is observed, $E_a^{des}(\Theta)=(55.8+1.1\times\Theta)$kcal/mol for initial coverages in the range 0.01–1 ML.

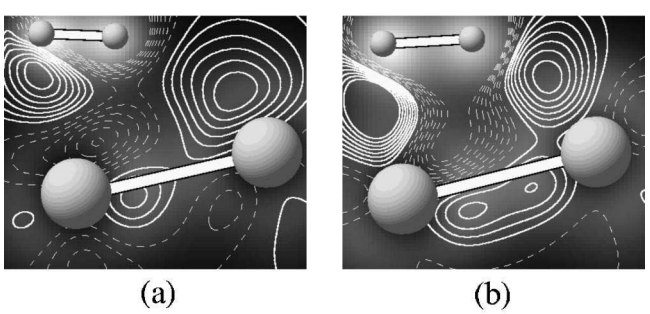

FIG. 6. Total valence electron density $n(\mathbf{r})$ (grey shading) and the density difference $\Delta n(\mathbf{r})$ (contour plot) in the plane containing the H_2 molecule and the Si-Si surface dimer at the TS geometries of the Si_9H_{12+2} (a) and the $Si_{21}H_{20+2}$ cluster (b) calculated with the PW91 functional. The density difference is defined by $\Delta n(\mathbf{r})=n(\mathbf{r})-n_{TS}^{clust}(\mathbf{r})-n_{TS}^{H_2}(\mathbf{r})$. The full contour lines correspond to $\Delta n>0$ and dashed lines to $\Delta n<0$. The plot levels are the same for both clusters.

TABLE IV. Coverage dependence of the reaction energy $E_{rxn}(\Theta)$ for the slab.

	$E_{rxn}(\Theta)$, kcal/mol (eV) per H_2		
	0.5 ML	1 ML	1→0.5 ML
LDA	48.1 (2.09)	49.7 (2.16)	51.3 (2.22)
BP	41.8 (1.81)	43.8 (1.90)	45.7 (1.98)
PW91	42.9 (1.86)	44.7 (1.94)	46.5 (2.02)
BLYP	42.9 (1.86)	44.3 (1.92)	45.7 (1.98)

The reaction energy E_{rxn} calculated with respect to the symmetric 2×1 reconstructed Si(001) surface shows very similar behavior. The respective $E_{rxn}(\Theta)$ values are increased by a few kcal/mol. In this case, when a H_2 molecule desorbs, it leaves behind a symmetric unoccupied dimer and therefore the final state is $\sim\Delta E$ higher in energy than for the buckled surface reconstruction.

V. CONCLUSIONS

We have presented a systematic *ab initio* study of the H_2/Si(001) reaction energetics employing three clusters in plane-wave DFT calculations. A five-layer $p(2\times2)$ slab was used as a reference to analyze the convergence of the cluster predictions. All calculations were performed within LDA and with the nonlocal BP, PW91 and BLYP exchange-correlation functionals. As our results show, a conservative conclusion can be drawn that the most frequently used Si_9H_{12} cluster is not large enough either to model the properties of the bare Si(001) surface or the molecular H_2 dissociation on it. The latter stems from the fact that this cluster is not capable of recovering the surface electronic structure. Though the H_2 reaction with the Si(001) surface is considered to be a highly localized event, nonlocal effects enter the reaction energetics via their influence on the surface bands. Hence, one could also expect different performance for the various functionals.

Our analysis shows that the quality of a given exchange-correlation functional should not be assessed without referring to the particular size of the cluster employed to study the H_2/Si(001) adsorption/desorption process. Indeed, it is evident, by inspecting the BLYP section of Table III for example, that one could infer for the Si_9 cluster an activation barrier to desorption much higher than the experimental values. Hence, as usually proceeded, the prepairing mechanism could be ruled out on energetic grounds. Such a conclusion, however, seems to be premature if one refers to the slab or, eventually, the Si_{21} cluster prediction within the same functional.

In contrast to the one-dimer cluster approximation, the $Si_{21}H_{20}$ cluster was found to be close in its predictions to the

slab calculations in all aspects of the reaction considered. With $E_a^{\mathrm{des}} = 56 \pm 3$ kcal/mol it is also well within the range of the experimentally determined desorption barriers. The relatively large spread in the calculated energies comes from the functionals used, with the BLYP functional giving the largest value for $E_a^{\mathrm{ads,des}}$. ZPE corrections were not considered, but as they amount to a few kcal/mol at most and are essentially the same for different functionals, no qualitative change of our results is expected upon their inclusion. Concluding, our findings suggest that the effect of the cluster size in modeling the H_2 reaction with the Si(001) surface is significant and some of the previous works may well need a revision.

ACKNOWLEDGMENTS

One of the authors (E.P.) is much indebted to A. P. Seitsonen and M. Fuchs for the valuable discussions and help during this study. We are grateful to Dr. E. Pehlke for critical reading of the manuscript and suggestions.

[1] For a nice review, see D. J. Doren, *Advances in Chemical Physics*, edited by I. Prigogine and S. A. Rice (Wiley, New York, 1996), Vol. 95, p. 1; K. Kolasinski, Int. J. Mod. Phys. B **9**, 2753 (1995).
[2] K. Sinniah, M. G. Sherman, L. B. Lewis, W. H. Weinberg, J. T. Yates, Jr., and K. C. Janda, Phys. Rev. Lett. **62**, 567 (1989).
[3] M. L. Wise, B. G. Koehler, P. Gupta, P. A. Coon, and S. M. George, Surf. Sci. **258**, 166 (1991).
[4] U. Höfer, L. Li, and T. Heinz, Phys. Rev. B **45**, 9485 (1992).
[5] P. Nachtigall, K. D. Jordan, and C. Sosa, J. Phys. Chem. **97**, 11666 (1993).
[6] P. Nachtigall, K. D. Jordan, and K. C. Janda, J. Chem. Phys. **95**, 8652 (1991).
[7] C. J. Wu, I. V. Ionova, and E. A. Carter, Surf. Sci. **295**, 64 (1993).
[8] P. Nachtigall, K. D. Jordan, and C. Sosa, J. Chem. Phys. **101**, 8073 (1994).
[9] Z. Jing and J. Whitten, J. Chem. Phys. **98**, 7466 (1993).
[10] Z. Jing and J. Whitten, J. Chem. Phys. **102**, 3867 (1995).
[11] P. Nachtigall, K. D. Jordan, A. Smith, and H. Jónsson, J. Chem. Phys. **104**, 148 (1996).
[12] M. R. Radeke and E. A. Carter, Phys. Rev. B **54**, 11803 (1996); **55**, 4649 (1997).
[13] S. Pai and D. Doren, J. Chem. Phys. **103**, 1232 (1995).
[14] A. Vittadini and A. Selloni, Chem. Phys. Lett. **235**, 334 (1995).
[15] E. Pehlke and M. Scheffler, Phys. Rev. Lett. **74**, 952 (1995).
[16] P. Kratzer, B. Hammer, and J. K. Nørskov, Phys. Rev. B **51**, 13432 (1995).
[17] M. C. Flowers, N. B. H. Jonathan, Y. Liu, and A. Morris, J. Chem. Phys. **99**, 7038 (1993).
[18] P. Bratu, W. Brenig, A. Groß, M. Hartmann, U. Höfer, P. Kratzer, and R. Russ, Phys. Rev. B **54**, 5978 (1996).
[19] P. Nachtigall (unpublished); D. Doren (unpublished).
[20] A. D. Becke, Phys. Rev. A **38**, 3098 (1988).
[21] C. Lee, W. Yang, and R. G. Parr, Phys. Rev. B **37**, 785 (1988).
[22] J. P. Perdew, J. A. Chevary, S. H. Vosko, K. A. Jackson, M. R. Pederson, D. J. Singh, and C. Fiolhais, Phys. Rev. B **46**, 6671 (1992).
[23] J. P. Perdew, Phys. Rev. B **33**, 8822 (1986).
[24] P. J. Stephens, F. J. Devlin, C. F. Chabalowski, and M. J. Frisch, J. Phys. Chem. **98**, 11623 (1994); A. D. Becke, J. Chem. Phys. **98**, 5648 (1993).
[25] P. Nachtigall and K. D. Jordan, J. Chem. Phys. **102**, 8249 (1995).
[26] J. Dabrowski and M. Scheffler, Appl. Surf. Sci. **56–58**, 15 (1992).
[27] R. A. Wolkow, Phys. Rev. Lett. **68**, 2636 (1992).
[28] W. Brenig, A. Gross, and R. Russ, Z. Phys. B **96**, 231 (1994).
[29] M. C. Flowers, N. B. H. Jonathan, A. Morris, and S. Wright, J. Chem. Phys. **108**, 3342 (1998).
[30] M. Bockstedte, A. Kley, J. Neugebauer, and M. Scheffler, Comput. Phys. Commun. **107**, 187 (1997); see also http://www.fhi-berlin.mpg.de/th/fhimd/code.html.
[31] D. M. Ceperley and B. J. Alder, Phys. Rev. Lett. **45**, 566 (1980).
[32] J. P. Perdew and A. Zunger, Phys. Rev. B **23**, 5048 (1981).
[33] M. Fuchs and M. Scheffler, Comput. Phys. Commun. (in press).
[34] D. R. Hamann, Phys. Rev. B **40**, 2980 (1989).
[35] M. Fuchs, M. Bockstedte, E. Pehlke, and M. Scheffler, Phys. Rev. B **57**, 2134 (1998).
[36] N. Troullier and J. L. Martins, Phys. Rev. B **43**, 1993 (1991).
[37] J. Dabrowski, E. Pehlke, and M. Scheffler, Phys. Rev. B **49**, 4790 (1994).
[38] I. V. Ionova and E. A. Carter, J. Chem. Phys. **98**, 6377 (1993).
[39] R. Konečný and D. J. Doren, J. Chem. Phys. **106**, 2426 (1997).
[40] C. Yang, S. Y. Lee, and H. C. Kang, J. Chem. Phys. **107**, 3295 (1997).
[41] B. Paulus, Surf. Sci. **408**, 195 (1998).
[42] N. Roberts and R. J. Needs, Surf. Sci. **236**, 112 (1990).
[43] P. Krüger and J. Pollmann, Phys. Rev. Lett. **74**, 1155 (1995).
[44] H. Over, J. Wasserfall, W. Ranke, C. Ambiatello, R. Sawitzki, D. Wolf, and W. Moritz, Phys. Rev. B **55**, 4731 (1997).
[45] E. Landemark, C. J. Karlsson, Y.-C. Chao, and R. I. G. Uhrberg, Phys. Rev. Lett. **69**, 1588 (1992); E. L. Bullock, R. Gunnella, L. Patthey, T. Abukawa, S. Kono, C. R. Natoli, and L. S. O. Johansson, *ibid.* **74**, 2756 (1995).
[46] E. Pehlke and M. Scheffler, Phys. Rev. Lett. **71**, 2338 (1993).
[47] L. S. O. Johansson, R. I. G. Uhrberg, P. Martensson, and G. V. Hansson, Phys. Rev. B **42**, 1305 (1990).
[48] J. E. Northrup, Phys. Rev. B **47**, 10032 (1993).
[49] Q. Liu and R. Hoffmann, J. Am. Chem. Soc. **117**, 4082 (1995).
[50] B. Hammer, K. W. Jacobsen, and J. K. Nørskov, Phys. Rev. Lett. **70**, 3971 (1993); B. Hammer, M. Scheffler, K. W. Jacobsen, and J. K. Nørskov, *ibid.* **73**, 1400 (1994).
[51] R. Konecny and D. J. Doren, J. Phys. Chem. B **101**, 10983 (1997).
[52] R. Konecny and D. J. Doren, J. Am. Chem. Soc. **119**, 11098 (1997).
[53] For $E_{\mathrm{rxn}}(\Theta)$ in case of hydrogen chemisorption on vicinal Si(001) surfaces, a very similar coverage dependence was calculated, see E. Pehlke and P. Kratzer, Phys. Rev. B **59**, 2790 (1999).